JGR Oceans

RESEARCH ARTICLE
10.1029/2022JC018405

Inorganic Carbon Transport and Dynamics in the Florida Straits

Yuan-Yuan Xu[1,2], Rik Wanninkhof[2], Emily Osborne[2], Molly Baringer[2], Leticia Barbero[1,2], Wei-Jun Cai[3], and James Hooper[1,2]

[1]Rosenstiel School for Marine, Atmospheric and Earth Science, Cooperative Institute for Marine and Atmospheric Studies, University of Miami, Miami, FL, USA, [2]NOAA Atlantic Oceanographic and Meteorological Laboratory, Miami, FL, USA, [3]School of Marine Science and Policy, University of Delaware, Newark, DE, USA

Key Points:

- Short-term variations in surface water oxygen and dissolved inorganic carbon concentrations are strongly influenced by the Florida Current transport
- Anthropogenic carbon accumulation and dissolved oxygen decrease are two main factors that lead to the long-term increase in dissolved inorganic carbon of the Florida Straits
- The highest long-term rate of increase in dissolved inorganic carbon of North Atlantic Central Water is likely due to the highest rate of increase in respiration

Supporting Information:

Supporting Information may be found in the online version of this article.

Correspondence to:

Y.-Y. Xu and R. Wanninkhof,
yyx@udel.edu;
rik.wanninkhof@noaa.gov

Citation:

Xu, Y.-Y., Wanninkhof, R., Osborne, E., Baringer, M., Barbero, L., Cai, W.-J., & Hooper, J. (2022). Inorganic carbon transport and dynamics in the Florida Straits. *Journal of Geophysical Research: Oceans*, *127*, e2022JC018405. https://doi.org/10.1029/2022JC018405

Received 2 JAN 2022
Accepted 20 SEP 2022

Abstract Ocean heat and carbon are transported through the Florida Straits, contributing to the Atlantic Meridional Overturning Circulation, and playing an important role in climate. Insufficient observations of carbonate chemistry within the Florida Straits have limited our understanding of ocean acidification within this region. To examine carbonate chemistry and carbon transport dynamics within this region, we developed an algorithm to estimate dissolved inorganic carbon (DIC) using more routinely measured input parameters (temperature, salinity, and dissolved oxygen [DO]) and the corresponding sampling date, depth, and longitude. The developed DIC algorithm output demonstrates good agreement with limited existing in situ observations. By applying this algorithm, we developed a seasonally resolved time series of DIC spanning from 2002 to 2018 for the Florida Straits at 27°N. This time series suggests that short-term variations in surface water DO and DIC were strongly influenced by the Florida Current transport. The long-term increase in DIC was mainly caused by anthropogenic carbon accumulation and DO decrease. The highest increasing rate in DIC was found in North Atlantic Central Water where DO decrease was fastest while the decreasing rate in pH was highest in Antarctic Intermediate Water (AAIW) because of the lower buffer capacity of this water mass. The long-term pH decrease, especially in AAIW, can impact the health of deep corals in the Florida Straits. Quantifying carbon transport between the coast of Florida and the Bahamas is important to understanding the carbonate chemistry dynamics and the long-term acidification of this important region.

Plain Language Summary A large amount of ocean heat and carbon is transported northward through the Florida Straits, the upper limb of the Atlantic Meridional Circulation, and plays a role in ocean carbonate chemistry along the U.S. east coast. Our understanding of carbon transport and ocean acidification in the Florida Straits is limited by insufficient carbonate chemistry data within this region. To address this issue, we developed an algorithm based on high-quality data from carbonate chemistry-focused research cruises. Then we applied this algorithm to seasonally resolved hydrographic time-series data from 2002 to 2018 to generate the carbonate chemistry datasets for the study region. We found that short-term variation in surface water dissolved oxygen was strongly correlated with volume transport. During the past two decades, dissolved oxygen showed a significant decreasing trend, and dissolved inorganic carbon showed a significant increasing trend. In addition, the increasing rate of dissolved inorganic carbon was highest in North Atlantic Central Water where the decreasing rate in dissolved oxygen was greatest. Furthermore, the long-term declines in pH and aragonite saturation state have the potential to threaten the health of corals living in the Florida Straits.

1. Introduction

The North Atlantic Ocean plays an important role in the uptake of anthropogenic CO_2 and the global carbon cycle (Friedlingstein et al., 2022; Sarmiento et al., 1995; Takahashi et al., 2009). The northward carbon flux through the Florida Straits is a major contributor to the North Atlantic Ocean carbon budget (Rosón et al., 2003). The quantification of natural and anthropogenic carbon transport across the Florida Straits contributes to the estimation and understanding of the North Atlantic and global carbon budget (Brown et al., 2021; Rosón et al., 2003).

In the Florida Straits, the Florida Current passes through productive and diverse marine ecosystems, including extensive shallow and deep coral reef ecosystems (Lee et al., 1992; Schmitz & Richardson, 1991; Sponaugle et al., 2005). Therefore, understanding both the physical and chemical dynamics in the Florida Straits has important biological and ecosystem implications. Within our study region, recent numerical model results suggest that

deep-coral habitats along the western side of the Florida Straits are strongly influenced by the movement of deep waters and by the properties of source waters on weekly to monthly timescales (Jiang et al., 2020). However, the long-term changes in the carbonate system and impacts on local ecosystems have not been well-studied, largely due to the lack of historical carbonate chemistry observations for the Florida Current (Wanninkhof et al., 2019; Zhang & Woosley, 2021). Extensive research on ocean acidification (OA) and the associated redistribution of dissolved inorganic carbon (DIC) species (increase in bicarbonate ion and decrease in carbonate ion concentration) has shown negative impacts on calcification by marine organisms such as corals and shellfish (Cohen & Holcomb, 2009; Hoegh-Guldberg et al., 2007; Mollica et al., 2018). OA can also affect marine organism physiology and function and has the potential for cascading impacts on marine food webs (Boulais et al., 2017; Jin et al., 2020; Kaniewska et al., 2012; Whiteley, 2011).

In this study, we investigate the carbonate chemistry dynamics between Florida and the Bahamas at 27°N, where the hydrography is dominated by the Florida Current (Wennekens, 1959). Extensive hydrographic datasets have been collected at 27°N for several decades, and a limited number of carbonate chemistry measurements has been collected from several cruises since 1998. Long-term physical oceanographic monitoring of the Florida Current transport at the Florida Straits was established in 1982 and includes a submarine telephone cable that is used to determine the water transport changes across the Florida Straits (Baringer & Larsen, 2001). Ship-based hydrographic observations are collected approximately three to four times per year across the Florida Straits at 27°N since 2001, in part to calibrate the cable measurements (Garcia & Meinen, 2014).

In order to generate a long-term carbonate chemistry record at the seasonal frequency of ship-based hydrographic surveys for the Florida Straits at 27°N, we employ an indirect approach to reconstruct carbonate chemistry parameters using the available hydrographic and oxygen time-series data (Table S1 in Supporting Information S1). In this study, we develop an algorithm to estimate DIC using data obtained from carbonate chemistry focused research surveys across the Florida Straits at 27°N. This algorithm is then applied to the long-term non-carbonate chemistry time-series data set (temperature, salinity, dissolved oxygen (DO), date (including the year), depth, and longitude) to generate a DIC record. From this DIC record, we also calculate commonly reported OA variables, pH and aragonite saturation state (Ω_{arag}), using a combination of salinity-derived total alkalinity (TA), temperature, salinity, and pressure. Importantly, our algorithm includes time-dependent variable information and thus is beyond other algorithms for generating climatology variables. Together, these carbonate chemistry records are used to characterize the interannual dynamics and long-term trend of OA in the Florida Straits region.

2. Methods

2.1. Study Region

The Florida Straits is a chokepoint with all Florida Current waters passing through an approximately 100 km corridor between Florida and the Bahamas (Baringer & Larsen, 2001; Beal et al., 2008; Larsen & Sanford, 1985; Leaman et al., 1987). The Florida Current is of South Atlantic and Caribbean Sea origin and flows northward between Florida Straits and Cape Hatteras (Larsen, 1992). It transports heat, contributes to the Atlantic Meridional Overturning Circulation (AMOC), and plays an important role in climate change (Lynch-Stieglitz, 2017; McCarthy et al., 2015). Due to the high-volume transport of the Florida Current through the Florida Straits, the characteristics of this water mass can influence distant coastal and ocean systems downstream along the East Coast of the US and the North Atlantic.

There are three major water masses in the Florida Straits (Figure 1). In this study, we followed the classification methods of Szuts and Meinen (2017) and Brown et al. (2021) and defined the three water masses as surface water (SW, potential density (σ_θ) < 24.0 kg m^{-3}), the North Atlantic Central Water (NACW, 24.0 < σ_θ < 27.2 kg m^{-3}), and Antarctic Intermediate Water (AAIW, σ_θ > 27.2 kg m^{-3}). SW is warm and moderately salty (Szuts & Meinen, 2017), the NACW is salty and primarily comprised of subtropical North Atlantic water (Schmitz & Richardson, 1991), and the AAIW is cold and fresh (Talley et al., 2011).

2.2. Surface Mixed Layer DIC

Surface mixed layer (depth <50 m) DIC for the Florida Straits at 27°N was calculated from CO2SYS (Van Heuven et al., 2009) using derived the fugacity of carbon dioxide (fCO_2) and TA data provided in the monthly averaged

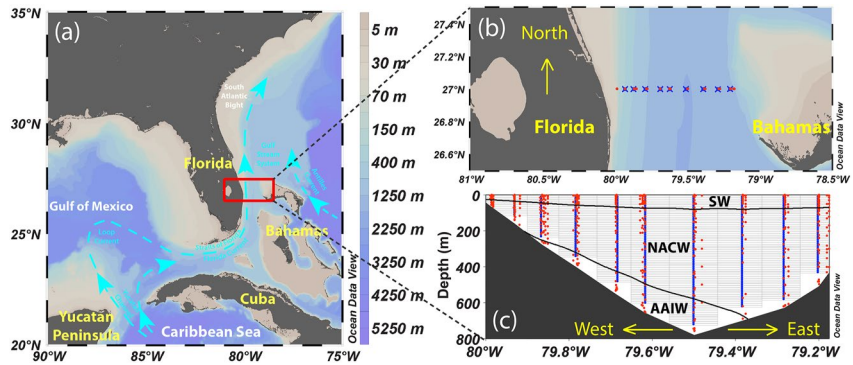

Figure 1. (a) Map showing regional bathymetry and major current systems near the Florida Straits (modified from Morey et al., 2017). The red box highlights the 27°N transect across the Florida Straits. (b) Surface view of the study region with red dots representing sampling locations for the carbonate chemistry measurements (dissolved inorganic carbon [DIC], total alkalinity [TA], and pH) and blue crosses representing seasonal sampling locations of hydrographic parameters (temperature, salinity, velocity) and dissolved oxygen (DO). (c) Section view of the 27°N transect with dots showing the depths of available carbonate chemistry and hydrographic parameters. The section has been divided into boxes (in gray) for the calculations of volume transport and DIC transport.

mapped product by Wanninkhof et al. (2020) at 1° × 1° spatial resolution from 2002 to 2018. The average mixed layer depth from 2002 to 2018 for the Florida Straits at 27°N was 41.4 m based on the data products provided by Wanninkhof et al. (2020). In this study, we used a cutoff depth of 50 m for the surface mixed layer and applied the calculations of surface mixed layer DIC to 10, 20, 30, and 40 m of the water column. Note that the short-term change in the mixed layer depth could potentially influence the values of carbonate chemistry parameters for water column between the actual mixed layer depth and 50 m. No long-term trend was observed in the mixed layer depth.

The anthropogenic carbon increase for the surface mixed layer was estimated following a disequilibrium method for the mixed layer proposed by Brown et al. (2021) where the DIC difference was calculated from TA and fCO_2 at the time of year (Wanninkhof et al., 2020) and fCO_2 at the year of 1998. The reference year 1998 was chosen because it is the first year that high-quality DIC was obtained in the Florida Straits at 27°N. fCO_2 measurements at the year of 1998 for the region with a longitude between −80°W and −79°W and a latitude near 27°N came from four cruises conducted in January, February, July, and November of 1998 on board the NOAA Ship *Ronald H. Brown* (https://www.aoml.noaa.gov/ocd/ocdweb/brown/brown_1998.html). fCO_2 data in other months of 1998 were estimated by interpolating the available measured data from the 4 months to all months using the average seasonal cycle for 2002–2018.

2.3. Data Source for Subsurface DIC Estimation

A total of 10 research cruises surveyed carbonate chemistry along the Florida Straits 27°N transect over the past two decades (Table 1). The earliest data set was collected in February 1998 during the World Ocean Circulation Experiment Hydrographic Program (WOCE/WHP), now called GO-SHIP, A05 line cruise. The A05 line was repeated several times since 1998. Data from the A05 line cruise that was conducted in 2004 were not used in this study due to the lack of temperature data. The 27°N Florida Straits transect was not surveyed by the A05 line cruise that was conducted in 2010 so data from this cruise was not used. Data from the A05 line cruise that was conducted in 2015 (A05-15) was used. The other carbonate chemistry data were collected during three Gulf of Mexico Ecosystem and Carbon Cycle (GOMECC) cruises (GOMECC-1 in July 2007, GOMECC-2 in July 2012, and GOMECC-3 in August 2017), two East Coast Ocean Acidification (ECOA) cruises (ECOA-1 in July 2015 and ECOA-2 in July 2018), and two Western Boundary Time Series cruises on the NOAA Ship *Ronald H. Brown* (RB-03 and RB-06 in February 2003 and March 2006).

Temperature, salinity, and pressure data collected on GO-SHIP, GOMECC, and ECOA cruises were measured with a Conductivity-Temperature-Depth (CTD) system at 1-m resolution. CTD salinity data have been corrected using onboard bottle salinity measurements. DO, DIC, and TA were measured onboard at sea using seawater collected from Niskin bottles at discrete depths (red dots in Figure 1c) from the CTD/Rosette system. DO was measured using the Winkler titration method (Carpenter, 1965), DIC was measured using coulometric titration

Table 1
List of Cruises That Were Used for Algorithm Development and Validation

Cruise name	Sampling year	Sampling month	Variables measured	Algorithm development	Algorithm validation
A05-98	1998	February	T, S, O_2, DIC, TA	√	
RB-03	2003	April	T, S, DIC		√
A05-04	2004	April	S, DIC, TA		
RB-06	2006	March	T, S, DIC, TA		√
GOMECC-1	2007	July	T, S, O_2, DIC, TA	√	
GOMECC-2	2012	July	T, S, O_2, DIC, TA	√	
ECOA-1	2015	July	T, S, O_2, DIC, TA	√	
A05-15	2015	December	T, S, O_2, DIC, TA		√
GOMECC-3	2017	August	T, S, O_2, DIC, TA		√
ECOA-2	2018	July	T, S, O_2, DIC, TA	√	

Note. T, S, and O_2 represent temperature, salinity, and bottle oxygen, respectively.

(Johnson et al., 1993), and TA was measured by acidimetric titration following the methods described in Dickson et al. (2007). The accuracy and precision of DO measurement are ±0.3 and ±0.15 μmol kg^{-1} (Langdon, 2010). DIC and TA measurements were calibrated using the Certified Reference Material (Dickson, 2001: Dickson et al., 2007). The overall accuracy and precision of DIC and TA measurements are ±2 and ±3 μmol kg^{-1}, respectively.

Bottle DO data were not available for RB-03 and RB-06 cruises. In addition, TA data were not available for RB-03 cruise. Therefore, RB-03 and RB-06 data were not used for algorithm development but rather for validation. A05-15 data were also not used for algorithm development but rather for validation due to the short time interval between A05-15 (2015) and ECOA-1 (2015) cruise (Table 1). Similarly, GOMECC-3 data were also not used for algorithm development but rather for validation due to the short time interval between GOMECC-3 (2017) and ECOA-2 (2018) cruises (Table 1). Therefore, quality-controlled survey data from five research cruises (A05-98, GOMECC-1, GOMECC-2, EOCA-1, and ECOA-2) were used to develop a multiple linear regression (MLR) algorithm to estimate DIC based on temperature, salinity, DO, date, depth, and sampling longitude, which are parameters routinely measured during ship-based surveys across the Florida Straits at 27°N since 2001. Measurements collected across the water column, with the exception of the upper 50 m, were utilized in our algorithm development. The surface layer (0–50 m) was excluded to eliminate data where air-sea gas exchange of oxygen and CO_2 occur at different rates and are therefore not well-represented by the algorithm. For algorithm validation, DO data collected by optode sensors were used to calculate DIC when bottle DO data were not available.

For the algorithm application and reconstruction portion of this study, we utilized a nearly seasonally resolved ship-based time series comprised of a total of 63 cruises (2002–2018, as part of the Western Boundary Time Series project) collected across the Florida Straits at 27°N (supporting information Table S1; Garcia & Meinen, 2014). The 27°N transect sampling consisted of nine stations at 10-m vertical depth intervals for the entire water column sampled for temperature, salinity, velocity, and DO. Temperature was measured by a Sea-Bird Electronics, Inc (SBE) 3 sensor with a typical accuracy of ±0.004°C and salinity was measured by a SBE 4 sensor with a typical accuracy of ±0.0003 S m^{-1} per month and resolution of 0.00004 S m^{-1} at 24 scans per second. DO was measured by a SBE 43 polarographic sensor. Velocity was determined from lowered acoustic Doppler current profiler with an estimated accuracy of 3.7 cm s^{-1} (Garcia & Meinen, 2014). All utilized DO data collected by CTD electronic sensor data were calibrated using bottle measurements by minimizing the residuals between CTD data and bottle data using a non-linear least squares fitting procedure. The DO data from 2001 to 2003 were excluded due to the lack of usable bottle data for calibration (see the statements in NOAA Data Reports; https://doi.org/10.7289/V5/DR-AOML-72; https://doi.org/10.7289/DR-AOML-70).

2.4. Subsurface DIC Estimation and Full Carbonate System Calculation

Subsurface (depth ≥50 m) DIC signatures are a combination of the natural variability of DIC due to variations in biological and physical processes (DIC_{var}) and the relative change in anthropogenic DIC (ΔDIC_{ant}) to the reference year 1998.

Table 2
Coefficients and Statistics for Equations 1–4

ΔDIC_{ant}	α_0	−2001.76
	α_1	1.04091
	α_2	19.2221
	α_3	−14.7092
	α_4	−75.3006
	R^2	0.837
	RMSE	4.76
DIC_{var}	β_0	1131.85
	β_1	−10.4788
	β_2	35.4297
	β_3	−0.624679
	R^2	0.995
	RMSE	4.56
DIC	R^2	0.987
	RMSE	6.54

Note. The unit of RMSE is μmol kg^{-1}.

$$DIC = DIC_{var} + \Delta DIC_{ant} \quad (1)$$

Subsurface ΔDIC_{ant} was first determined separately for each cruise based on the differences between linear regression fits on temperature, salinity, and DO data from the A05-98 cruise (1998) and later cruises (GOMECC and ECOA cruises in 2007, 2012, 2015, and 2018) following the extended MLR (eMLR) method established by Friis et al. (2005). The eMLR method calculated anthropogenic CO_2 by subtracting coefficients of two fits rather than by the difference of two MLR fits (Friis et al., 2005). Individual MLR was developed for each cruise and the coefficients are given in supporting information Table S2 in Supporting Information S1. This provides the ΔDIC_{ant} between 1998 and 2007, 2012, 2015, and 2018. Next, the calculated ΔDIC_{ant} values were fitted with a MLR algorithm. The fit assumes that the ΔDIC_{ant} in the Florida Straits at 27°N accumulates over time while the rates vary with depth (positive numbers) and longitude difference with respect to −79.567°W, the center point of the section (ΔLongitude):

$$\Delta DIC_{ant} = \alpha_0 + \alpha_1 \times Date + \alpha_2 \times \ln(Depth) + \alpha_3 \times \Delta Longitude + \alpha_4 \times \Delta Longitude^2 \quad (2)$$

where α_0, α_1, α_2, α_2, and α_4 are coefficients that are determined by the best fit of Equation 2. These predictors were chosen based on the variation pattern of ΔDIC_{ant} with depth and longitude (supporting information Figure S1 in Supporting Information S1).

Subsurface DIC_{var} for each cruise was then calculated as the difference between measured DIC and ΔDIC_{ant}. The DIC_{var} values from GOMECC and ECOA cruises were fitted to a single MLR using predictors temperature, salinity, and DO,

$$DIC - \Delta DIC_{ant} = DIC_{var} = \beta_0 + \beta_1 \times Temperature + \beta_2 \times Salinity + \beta_3 \times DO \quad (3)$$

where β_0, β_1, β_2, and β_3 are coefficients that are determined by the best fit of Equation 3.

One major assumption of MLR method is that the parameters in the model are not collinear. To test this assumption, we calculated the variance inflation factors (VIFs) to quantify how much the variance is inflated due to collinearity of predictors. VIFs of predictors in Equation 2 are 6.9, 3.4, and 4.2 for Temperature, Salinity, and DO, respectively. VIFs of predictors in Equation 3 are 1.0, 1.2, 1.2, and 1.3 for Date, ΔLongitude, ln (Depth), and ×ΔLongitude^2, respectively. VIFs of all predictors in Equations 2 and 3 are less than 10, suggesting no potentially interfering collinearity (Franke, 2010).

Combining Equations 2 and 3, the subsurface DIC was estimated using temperature, salinity, DO, date (in decimal format, e.g., 2002.184), depth (positive numbers), and ΔLongitude (negative numbers on the western side and positive numbers on the eastern side of the center point) in the following form:

$$DIC = \alpha_0 + \alpha_1 \times Date + \alpha_2 \times \ln(Depth) + \alpha_3 \times \Delta Longitude + \alpha_4 \times \Delta Longitude^2 + \beta_0 + \beta_1 \times Temperature + \beta_2 \times Salinity + \beta_3 \times DO \quad (4)$$

The coefficients and statistics for the above equations are given in Table 2.

The MLR in Equation 4 was then applied to the 2002–2018 27°N transect hydrographic data set to generate a 16-year seasonally resolved DIC time series. The application of the MLR algorithms assumes physical mixing and biological activities are major drivers of the variations in carbonate chemistry parameters since the water parcels last contact with the atmosphere (Alin et al., 2012; Friis et al., 2005).

The salinity-TA linear relationship given in Equation 5 (Figure S2 in Supporting Information S1) was developed using the subsurface salinity and high-quality TA data collected from the A05-98, GOMECC, and ECOA cruises and used in this study.

$$TA = 48.966(\pm 0.559) \times salinity + 600.03(\pm 20.14) \quad (5)$$

The total number of observations used in Equation 5 was 261. The coefficient of determination (R^2) and the root mean square error (RMSE) of this linear regression were 0.967 and 5.97 μmol kg^{-1}, respectively. *F*-test on the linear regression expressed by Equation 5 was performed and this linear fit was significant with a *p*-value less than 0.05.

Subsurface DIC estimates and salinity-derived TA were used to calculate the remaining carbonate system parameters, including pH (in total hydrogen ion concentration scale) and Ω_{arag} using CO2SYS (Van Heuven et al., 2009). Within CO2SYS, we utilized the first and second carbonic acid dissociation constants in seawater (K_1 and K_2) from Lueker et al. (2000), the acidity constant of the ion HSO_4^- from Dickson (1990), and borate-to-salinity ratio determined by Lee et al. (2010). Ancillary hydrographic data including temperature, salinity, and pressure were also used for CO2SYS calculations. Note that nutrients data were not used in CO2SYS calculations for consistency because these data were not available in the seasonally resolved ship-based datasets.

Gridded long-term surface carbonate chemistry system data, including seawater fCO_2, pH, and Ω_{arag}, from 2002 to 2019 for the Florida Straits have been provided by Wanninkhof et al. (2020) using the observational data from the AOML Ship of Opportunity-CO_2 (SOOP-CO_2) program from Royal Caribbean international cruise ships and MLRs. However, SOOP-CO_2 data only covers observations measured for the surface mixed layer. Together with the carbonate chemistry data for the subsurface waters provided by this study, the carbonate system dynamics across the entire Florida Straits water column can thus be analyzed and explored.

2.5. Calculations of Volume Transport and DIC Transport

The calculated volume transport for each sampling box (at 10-m vertical depth intervals for the entire water column, Figure 1c), which includes one sampling location per box, was determined by multiplying the northward velocity and the corresponding area.

$$\text{Volume transport (Sv)} = \text{Velocity (cm/s)} \times \text{Area } \left(\text{m}^2\right) / 10^8 \tag{6}$$

Velocity was measured for each sampling box (see Section 2.2 for details). Vertical-section area for each sampling box was calculated according to the coordinates and depth coverage. The volume transport for the entire transect of the Florida Straits at 27°N (80–79.175°W) was then calculated by summing the volume transport values for all sampling boxes. Similarly, DIC transport for each sampling box was calculated first using the corresponding volume transport and DIC concentration. Then the total DIC transport of the Florida Straits at 27°N was calculated by the sum of the DIC transport values for all sampling boxes. The errors in DIC transport for the entire water column range from 1.10 Pg C yr^{-1} to 2.72 Pg C yr^{-1}.

2.6. Uncertainty Estimation

The overall uncertainty of the MLR algorithm (*E*) for subsurface DIC estimation was calculated following Carter et al. (2016) using the error in the measured response variable (E_{DIC}), the errors in measured predictors ($E_{predictor}$), and RMSE of the MLR algorithm (E_{MLR}).

$$E = \sqrt{E_{DIC}^2 + E_{predictor}^2 + E_{MLR}^2} \tag{7}$$

$E_{predictor}$ was calculated as $\sqrt{\sum_{j=1}^{n} (U_j \times \text{Coefficient}_j)^2}$, where U_j and Coefficient_j are the uncertainty and coefficient of the *j*th measured predictor used in the MLR algorithm. Uncertainties of 0.005°C, 0.005, and 0.3 μmol kg^{-1} for Temperature, Salinity, and DO were used in the calculation of $E_{predictor}$. E_{DIC} is 2 μmol kg^{-1} and E_{MLR} is 6.54 μmol kg^{-1}. As a result, the overall model uncertainty is 6.84 μmol kg^{-1}.

Errors in salinity-derived TA and MLR algorithm-estimated DIC lead to greater errors in calculated pH and Ω_{arag}. We estimated errors in our calculated pH and Ω_{arag} values using a Monte Carlo error analysis approach, which repeats random sampling of input parameters (TA and DIC) around their mean with respect to their uncertainties (5.97 μmol kg^{-1} for TA and 6.84 μmol kg^{-1} for DIC) for 1000 times to obtain the errors for the calculated parameters (pH and Ω_{arag}). The errors in pH range from 0.007 to 0.016 and the errors in Ω_{arag} range from 0.034 to 0.059.

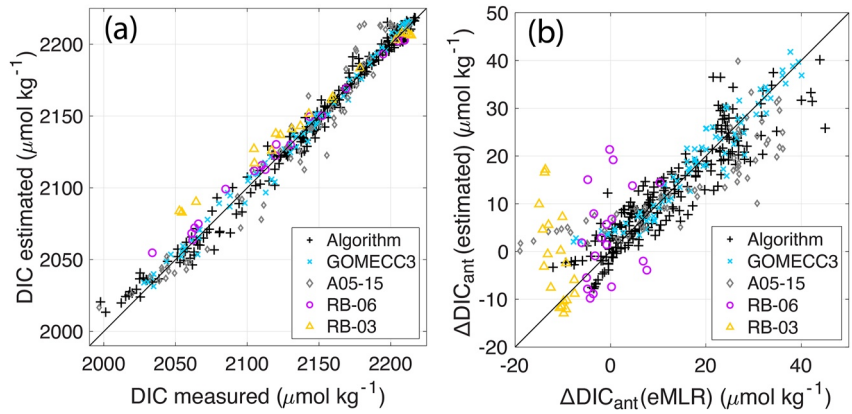

Figure 2. Scatterplots of (a) multiple linear regression (MLR) estimated dissolved inorganic carbon (DIC) versus measured DIC and (b) ΔDIC_{ant} calculated separately following the extended MLR method (Friis et al., 2005) versus the estimated ΔDIC_{ant} using an algorithm for combined data. The black cross symbols represent bottle data that are used for algorithm development. The black 1:1 line represents where estimation equals measurement.

2.7. Trend Analysis

Short-term variations and long-term changes in temperature, salinity, DO, DIC, volume transport, DIC transport, and ΔDIC_{ant} transport for the full water column were determined using observations (temperature, salinity, DO, and volume transport from repeated seasonal hydrographic focused surveys) and reconstructed data (DIC, DIC transport, and ΔDIC_{ant} transport) during 2002–2018. Note that the results for AAIW were possibly biased because of the incomplete spatial coverage by sampling locations for this water mass (Figure 1). To determine the long-term trends, linear regressions were performed using the reconstructed time series data during 2002–2018 and *p*-values for the *F*-test on the linear regressions were calculated to examine if a trend is significant or not.

2.8. Correlation Analysis

To examine the correlations between hydrographic and carbonate chemistry parameters, correlation analyses were performed for time series of two selected parameters. When examining short-term variabilities, any existing long-term linear trends in the reconstructed time series were removed before performing the correlation analysis to isolate decadal variabilities. To do this, linear regressions were first performed on the reconstructed time series and then were removed by subtracting the linear fits from those reconstructed time series.

2.9. Buffer Factor Calculation

Buffer factors were calculated to help explain the differences in the long-term trends of carbonate chemistry parameters in different water masses following two steps. First, species concentrations and thermodynamic constants were extracted from CO2SYS using the input pair of DIC and TA. Second, the acid-base buffer factors were calculated using the equations given in Table 2 of Egleston et al. (2010) with editing errors in the paper corrected by Álvarez et al. (2014).

3. Results

3.1. Algorithm Performance and Carbonate System Calculation Error

To assess the subsurface DIC algorithm performance, measured and estimated DIC values were compared and showed a strong 1:1 correlation (Figure 2). For data from GOMECC and ECOA cruises that were used to develop the subsurface DIC algorithm, the R^2 and RMSE were 0.987 and 6.54 μmol kg^{-1} (Table 2), respectively, indicating a skillful algorithm. The overall uncertainty of the subsurface DIC estimation was 6.84 μmol kg^{-1}. As for ΔDIC_{ant} estimation, the R^2 and RMSE were 0.837 and 4.76 μmol kg^{-1}, respectively (Table 2, Figure 2b). Negative ΔDIC_{ant} values were mainly found in AAIW, indicating slight deficiencies in the algorithms or removal or transfer of anthropogenic carbon into other water masses (Iudicone et al., 2016).

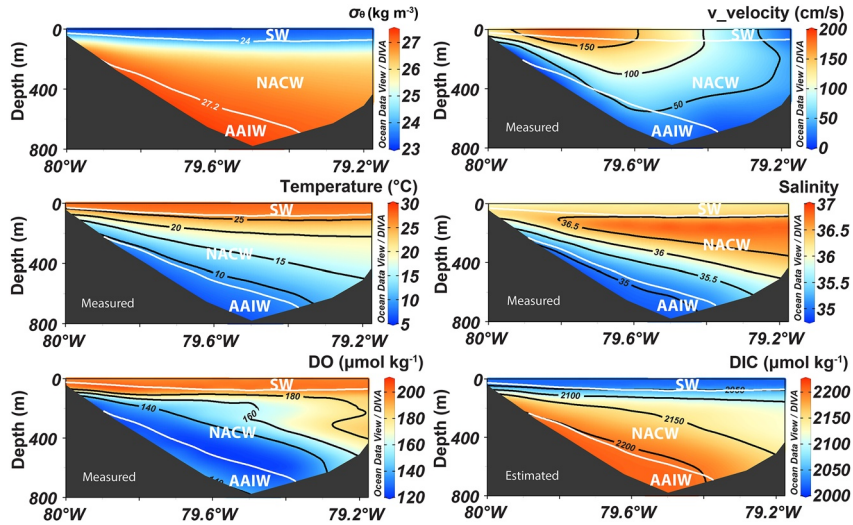

Figure 3. Mean states of (a) σ_θ, (b) northward alongshore velocity (v_velocity), (c) temperature, (d) salinity, (e) dissolved oxygen (DO), and (f) dissolved inorganic carbon (DIC) across the Florida Straits at 27°N. The averaged data for each parameter over 2002–2018 are presented. The black lines are contour lines for each parameter. The white lines that separate three major water masses (Surface Water [SW], North Atlantic Central Water [NACW], and Antarctic Intermediate Water [AAIW]) are shown on all panels. Whether a variable on the *y*-axis was measured or estimated is indicated by the white text on each panel.

Data from RB-03, RB-06, A05-15, and GOMECC-3 cruises, which were not used for algorithm development, were used for validation of the MLR algorithm. The corresponding biases and RMSEs of subsurface DIC for RB-03, RB-06, A05-15, and GOMECC-3 were 9.32 ± 14.2, 3.84 ± 7.70, −0.51 ± 14.14, and −0.74 ± 5.23 μmol kg^{-1}, respectively. The bias and RMSE for RB-03 cruise data were anomalous in comparison to the other cruise data and to the values that were used for subsurface DIC-algorithm development. The anomalous bias for RB-03 cruise data also existed when using the recently published Empirical Seawater Property Estimation Routines (ESPERs) by Carter et al. (2021). It was unclear why the MLR algorithm didn't fit the RB-03 data well but we hypothesized that it might be due to changes in water mass properties that occurred in 2003 (Figure S3 in Supporting Information S1).

3.2. Mean States and Long-Term Changes in Velocities and Carbon Parameters

The mean states of velocity and carbon parameters across the Florida Straits at 27°N were determined by averaging observations (σ_θ, northward velocity, temperature, salinity, DO) and estimations (DIC) across the entire strait for each parameter over the past 16 years from 2002 to 2018. Temperature, salinity, DO, and DIC gradients were larger on the western side than those on the eastern side (Figure 3). SW was characterized by high temperature (27.39 ± 1.46°C), high DO (199.2 ± 6.1 μmol kg^{-1}), and low DIC (2028.3 ± 12.3 μmol kg^{-1}) (Figure 3). In contrast, AAIW was characterized by low temperature (7.63 ± 0.75°C), low DO (127.7 ± 6.3 μmol kg^{-1}), and high DIC (2209.8 ± 5.7 μmol kg^{-1}) (Figure 3). The dominant feature of NACW was the wedge-shaped high salinity area on the eastern side of the transect (Figure 3). In addition, the spatial variations in all parameters of NACW were larger than those of SW and AAIW and the change in DO with depth was non-linear (Figure 3).

For the full water column across the entire Florida Straits at 27°N, there were no significant trends in temperature and salinity, while DO was decreasing at a rate of −0.52 ± 0.12 μmol kg^{-1} yr^{-1} (Figure 4). Further, no significant trends were found in temperature and salinity of SW, NACW, or AAIW. Negative trends in DO were observed in NACW (−0.70 ± 0.16 μmol kg^{-1} yr^{-1}), AAIW (−0.22 ± 0.11 μmol kg^{-1} yr^{-1}), and SW (−0.43 ± 0.11 μmol kg^{-1} yr^{-1}) (Table 3).

However, there were trends of increasing temperature and salinity in the Florida Straits since 2012 as the AMOC ceased reducing further but rather increased slightly since 2012 (Smeed et al., 2018). Therefore, we broke down the period 2002–2018 into two periods 2002–2012 and 2012–2018 to further study the carbonate chemistry dynamics in the Florida Straits under the influence of AMOC. We observed significant positive trends ($p < 0.05$)

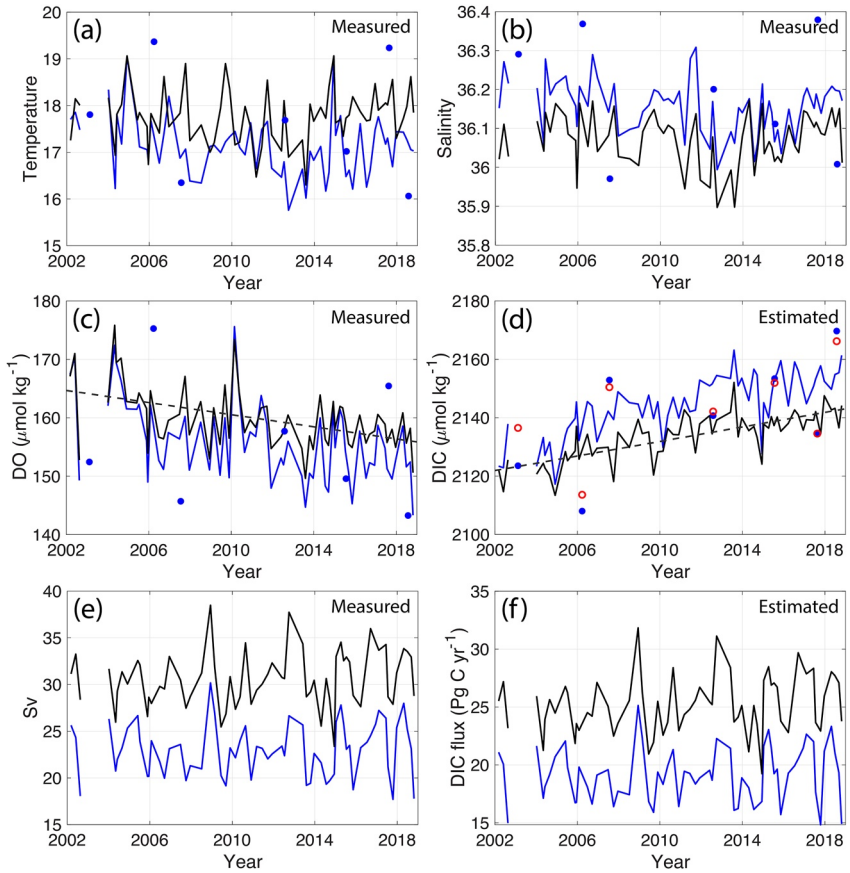

Figure 4. Temporal changes in full water column (black lines) and North Atlantic Central Water (NACW) (blue lines) measured (a) temperature, (b) salinity, and (c) dissolved oxygen (DO) from the ship-based time series, (d) calculated dissolved inorganic carbon (DIC), (e) volume transport, and (f) DIC transport across the Florida Straits at 27°N. The dashed lines represent linear trends. The blue dots represent measured values while the red open circles represent multiple linear regression estimated values for NACW averaged over locations where seawater samples were collected by Niskin bottles. Whether a variable on the *y*-axis was measured or estimated is indicated by the black text on each panel. Temporal changes for Surface Water and Antarctic Intermediate Water are provided in Figures S5 and S6 in Supporting Information S1.

Table 3
Changes of Temperature (Measured), Salinity (Measured), Dissolved Oxygen (DO) (Measured), Dissolved Inorganic Carbon (DIC), ΔDIC_{ant}, pH, Ω_{arag}, the Average Transports With Associated Standard Deviations of Water Mass Volume (Measured), DIC, and ΔDIC_{ant} (to the Reference Year 1998) During 2002–2018

	Overall	SW	NACW	AAIW
Temperature (°C yr^{-1})	0.010 ± 0.016*	0.058 ± 0.033*	−0.031 ± 0.016*	−0.006 ± 0.008*
Salinity (yr^{-1})	−0.0007 ± 0.0018*	−0.0051 ± 0.0027*	−0.0039 ± 0.0018	−0.0024 ± 0.0009
DO (μmol kg^{-1} yr^{-1})	−0.52 ± 0.12	−0.43 ± 0.11	−0.70 ± 0.16	−0.22 ± 0.11
DIC (μmol kg^{-1} yr^{-1})	1.23 ± 0.14	0.96 ± 0.16	1.62 ± 0.18	1.14 ± 0.06
ΔDIC_{ant} (μmol kg^{-1} yr^{-1})	1.04 ± 0.01	1.20 ± 0.12	0.99 ± 0.02	1.03 ± 0.02
pH (yr^{-1})	−0.0026 ± 0.0002	−0.0021 ± 0.0039	−0.0030 ± 0.0002	−0.0035 ± 0.0002
Ω_{arag} (yr^{-1})	−0.0115 ± 0.0021	−0.0061 ± 0.0017	−0.0172 ± 0.0024	−0.0094 ± 0.0007
Volume transport (Sv)	30.70 ± 2.97	6.40 ± 1.85	22.98 ± 2.84	1.32 ± 0.65
DIC transport (Pg C yr^{-1})	25.28 ± 2.68	5.03 ± 1.45	19.11 ± 2.34	1.14 ± 0.56
ΔDIC_{ant} transport (Pg C yr^{-1})	0.1351 ± 0.0646	0.0362 ± 0.0244	0.0997 ± 0.0477	−0.0008 ± 0.0028

Note. All trends in this table were statistically significant with *p*-values less than 0.05 except for those marked with the star symbols.

in both temperature and salinity in the measured data since 2012. The average temperature over the entire water column increased during 2012–2018 at a rate of 0.123 ± 0.056°C yr^{-1} and salinity increased during 2012–2018 at a rate of 0.023 ± 0.007 yr^{-1}.

The overall increasing rate in DIC for the entire water column across the entire Florida Straits at 27°N was 1.23 ± 0.14 μmol kg^{-1} yr^{-1} from 2002 to 2018 (Figure 4d). The increasing rate in DIC for NACW (1.62 ± 0.18 μmol kg^{-1} yr^{-1}) was higher than the overall rate while the increasing rate in DIC for AAIW (1.14 ± 0.06 μmol kg^{-1} yr^{-1}) was lower than the overall rate. As for SW, DIC increased at a rate of 0.96 ± 0.16 μmol kg^{-1} yr^{-1} from 2002 to 2018 (Table 3). In particular, the increasing rate in DIC for SW from 2012 to 2018 (1.91 ± 0.49 μmol kg^{-1} yr^{-1}) was higher than that from 2002 to 2012 (0.74 ± 0.41 μmol kg^{-1} yr^{-1}, p-value = 0.08). The accelerated DIC accumulation during 2012–2018 was concurrent with a salinity increase at a rate of 0.038 ± 0.008 yr^{-1}, while the salinity trend from 2002 to 2012 was not significant (Figure S4 in Supporting Information S1). During 2002–2018, ΔDIC_{ant} (to the reference year 1998) increased at an average rate of 1.04 ± 0.01 μmol kg^{-1} yr^{-1} (Table 3).

For the entire transect of the Florida Straits at 27°N, the overall rates of change for pH and Ω_{arag} were −0.0026 ± 0.0002 yr^{-1} and −0.0115 ± 0.0021 yr^{-1}, respectively. The rates of pH decline for the NACW (−0.0030 ± 0.0002 yr^{-1}) and the AAIW (−0.0035 ± 0.0002 yr^{-1}) were greater than the overall rate (−0.0026 ± 0.0002 yr^{-1}) while the rate of pH decline for SW (−0.0021 ± 0.0004 yr^{-1}) was lower than the overall rate (Table 3). During the same period, the rate for NACW Ω_{arag} decline (−0.0172 ± 0.0024 yr^{-1}) was higher than the overall rate while the SW Ω_{arag} rate (−0.0061 ± 0.0017 yr^{-1}) and AAIW (−0.0094 ± 0.0007 yr^{-1}) were both lower than the overall rate (Table 3).

No significant trends were found for volume and DIC transports during 2002–2018 (Figure 4). Volume transport of the Florida Straits at 27°N varied from 23.37 to 38.48 Sv with an average of 30.70 Sv during the period 2002–2018 (Figure 4e). The total volume transport increased slightly at a rate of 0.122 ± 0.077 Sv yr^{-1} but this trend was not statistically significant (p-value = 0.118, Figure 4e). The contribution of volume transport from NACW (22.98 Sv on average) was far greater than those from SW (6.40 Sv on average) and AAIW (1.32 Sv on average) (Table 3). The total DIC transport varied from 19.24 to 31.84 Pg C yr^{-1} with a mean value of 25.28 Pg C yr^{-1} (Figure 4f). The average contributions of DIC transport from the three major water masses were 5.03 Pg C yr^{-1} (SW), 19.11 Pg C yr^{-1} (NACW), and 1.14 Pg C yr^{-1} (AAIW), respectively (Table 3).

3.3. Short-Term Variability

The reconstructed time series clearly shows short-term variabilities in DO, DIC, and volume transport (Figure 4) where short-term refers to temporal change at seasonal resolution (~3 months). To examine relationships and the controlling mechanisms, correlation coefficients are calculated between any two of the three detrended data sets, in which their long-term linear trends have been removed so that the relationship analyses of their short-term variability are not distorted by long-term trends. For the entire water column at the Florida Straits 27°N transect, DIC has a strong relationship with DO ($r = -0.55$, $p < 0.01$) and 31% of the variation in DIC can be explained by this linear relationship.

The correlation analyses suggest that DO and DIC in SW and NACW and independently measured volume transport are significantly correlated (Figure 5). In SW, the linear correlation coefficients between detrended volume transport and DO and DIC are −0.51 and −0.56, respectively. In NACW, the linear correlation coefficients between detrended volume transport and DO and DIC are 0.36 and −0.36, respectively. These suggest that volume transport has a stronger correlation with short-term variability of DO and DIC in SW than in NACW. In AAIW, the linear correlation between detrended volume transport and DO is not statistically significant. The correlation coefficient between detrended volume transport and DIC is 0.37 for AAIW, suggesting that approximately 14% of the variation in DIC can be explained by the linear correlation between volume transport and DIC.

Similarly, the short-term variations of pH and Ω_{arag} in SW and NACW and independently measured volume transport are significantly correlated. In SW and NACW, the linear correlation coefficients between detrended volume transport and pH are −0.77 and 0.32, respectively. Linear correlation coefficients between detrended volume transport and Ω_{arag} are 0.57 and 0.31, respectively, for SW and NACW. For both DO and DIC, their relationships with volume transport are strongest in SW where the alongshore velocity is highest among three water masses. The same pattern holds true for pH and Ω_{arag}.

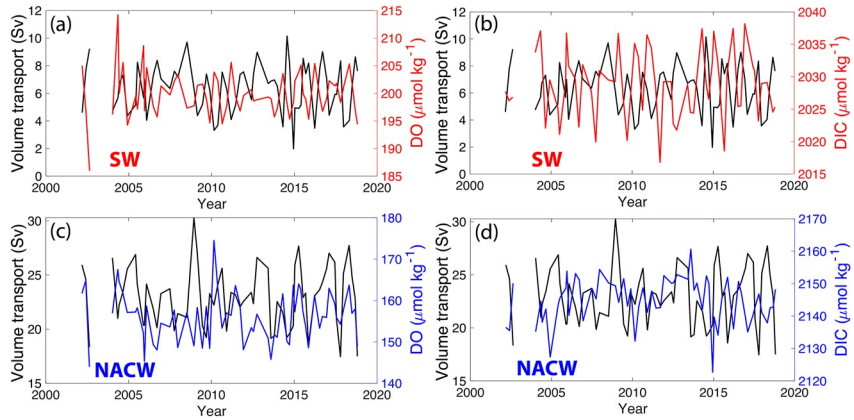

Figure 5. The relationships between detrended volume transport and (a) dissolved oxygen (DO) in Surface Water (SW), (b) dissolved inorganic carbon (DIC) in SW, (c) DO in North Atlantic Central Water (NACW), and (d) DIC in NACW in the Florida Straits at 27°N. Time series data have been detrended to remove their long-term linear trends and to show the short-term correlations between volume transport and other parameters. A similar figure using the original volume transport, DO, and DIC data is provided in Figure S7 in Supporting Information S1.

4. Discussion

4.1. Algorithm Development and Data Reconstruction

Previous studies generally calculated the carbon transport across the Florida Straits using carbonate chemistry data from a single cruise and volume transport data from model estimations or observations from one or few cruises (Brown et al., 2021; Macdonald et al., 2003; Rosón et al., 2003). To better quantify and characterize the carbon dynamics across the Florida Straits, our study uses in situ data from eight carbonate chemistry focused research cruises from 1998 to 2017 and hydrographic as well as velocity data from 63 cruises from 2002 to 2018 to fully capture the carbonate chemistry variations during the past two decades. By calculating carbonate chemistry data from temperature, salinity, and DO for water below the surface mixed layer across the Florida Straits at 27°N, this study also fills the long-term observational gap in carbonate chemistry variables below the surface mixed layer.

MLR approaches have been used to reconstruct carbonate system parameters based on empirical relationships between basic hydrographic parameters and the target carbonate system parameters developed using high-quality data obtained from limited cruises where both hydrographic and carbonate parameters are measured (e.g., Alin et al., 2012; McGarry et al., 2021). Regional MLR algorithms provide a means for reconstructing and characterizing carbonate chemistry dynamics where observations are sparse. However, the use of empirical relationships for reconstructing long-term (decadal or longer) carbonate chemistry data needs to be done with caution because the anthropogenic carbon increase over time is not accounted for when these algorithms are developed (Alin et al., 2012; McGarry et al., 2021). By using a MLR algorithm approach, our study is able to take into account the impact of anthropogenic carbon increase, which is particularly important for long-term reconstructions.

The recently published new global ESPER algorithms by Carter et al. (2021) quantified the impacts of anthropogenic carbon on DIC and pH with the implementation of a first-principles approach. We applied the ESPER-Mixed algorithm, which combines estimates from both linear regression and neural network estimates (Carter et al., 2021), to our validation data sets (RB-03, RB-06, A05-15, and GOMECC-3) using the same input parameters. The biases and RMSEs of subsurface DIC for RB-03, RB-06, A05-15, and GOMECC-3 are 12.67 ± 13.84, 4.19 ± 6.41, 4.83 ± 13.95, and 2.21 ± 5.70 μmol kg^{-1}, respectively. All these biases are higher than the values calculated using the regional algorithm developed for the Florida Straits in this study.

Several carbonate chemistry focused research cruises surveyed the Florida Straits at the 27°N transect since 1998, offering snapshots of the carbonate chemistry system in the Florida Straits at the time of sampling. However, these research cruises were conducted every few years and these surveys are seasonally biased as the earlier cruises (A05-98, RB-03, and RB-06) were conducted in January-March while the later cruises (GOMECC-1, GOMECC-2, GOMECC-3, ECOA-1, and ECOA-2) were conducted in July-August. Our reconstructed carbonate

chemistry data offer nearly seasonal temporal resolution and a uniform sampling interval (10-m depth interval at all stations) in terms of spatial coverage.

4.2. Long-Term Trends

A recent study by Brown et al. (2021) calculated the total anthropogenic carbon concentrations in the Florida Straits at 26.5°N for the period 2004–2012. Our study extends the temporal coverage by reconstructing carbonate chemistry data from 2002 to 2018 and estimates the relative change in ΔDIC_{ant} to the reference year 1998 rather than the total anthropogenic from pre-industrial era. The reference year 1998 is chosen because historical fCO_2 data collected from the first carbonate chemistry-focused research cruise in the Florida Straits at 27°N are available since 1998 for ΔDIC_{ant} calculation and measured fCO_2 data from the 1998 cruise are more accurate than the estimated pre-industrial era fCO_2 data. Compared with the total anthropogenic carbon transport in the Florida Straits provided by Brown et al. (2021), the average ΔDIC_{ant} transport since the reference year 1998 (0.135 Pg C yr^{-1}) accounts for approximately 21% of the total anthropogenic carbon transport since the pre-industrial era (0.634 Pg C yr^{-1}, Brown et al. (2021)), indicating that the fraction of anthropogenic carbon uptake is accelerating with time, in particular within the past two decades.

During 2004–2012, the overlapping period between the study by Brown et al. (2021) and this study, the mean volume transport at 27°N (30.31 Sv) of this study is similar to that at 26.5°N (31.58 Sv) given by Brown et al. (2021). However, the volume transport trends are in opposite directions as we see a slight increase (0.225 ± 0.188 Sv yr^{-1}, not statistically significant) in volume transport while Brown et al. (2021) found a decreased trend (-0.091 ± 0.062 Sv yr^{-1}) using data calculated by Smeed et al. (2014). This difference in the volume transport trend is likely due to the differences in temporal resolutions, methods, or data sets used in these two studies. In fact, no statistically significant trends in total transports of volume by the Florida Current have been observed during the past three decades (Meinen et al., 2010; Szuts & Meinen, 2017). As for 2002–2018, our results show that the volume transport increases slightly at a rate of 0.122 ± 0.077 Sv yr^{-1} but this trend is not statistically significant.

During the overlapping period 2004–2012, the increasing rate in ΔDIC_{ant} transport calculated in this study is lower than the one (17.0 ± 1.3 Tg C yr^{-2}) calculated by Brown et al. (2021). This difference in ΔDIC_{ant} transport can be attributed to the differences in the temporal coverage of bottle data used in the two studies. In particular, according to ΔDIC_{ant} estimates using the eMLR method, the increasing rate in ΔDIC_{ant} during 2004–2014 (2.25 ± 0.71 μmol kg^{-1} yr^{-1}) is much larger than that during 1998–2018 (1.25 ± 0.28 μmol kg^{-1} yr^{-1}, Figure S8 in Supporting Information S1). This study used bottle data that were collected during 1998–2018 for ΔDIC_{ant} calculation and therefore the increasing rate in ΔDIC_{ant} transport calculated in this study is lower than that of Brown et al. (2021).

The observed decrease of DO in SW can be explained by two reasons. First, SW (defined as potential density less than 24.0 kg m^{-3}, see Section 2.1) of the Florida Straits at 27°N consists of approximately 62.6% surface mixed layer water and 37.4% subsurface water below the surface mixed layer. The decreasing rate in DO of the subsurface SW is higher than those of the entire SW and the surface mixed layer water that is affected by air-sea gas exchange. Second, though not statistically significant, temperature of SW is increasing during 2002–2018 and contributes to DO decline as DO concentration is used for trend analysis.

Deoxygenation has been found in increasing areas of open ocean and coastal waters (Breitburg et al., 2018). For the entire water column of the Florida Straits at 27°N, a negative trend is observed in the measured DO data during 2002–2018. Results from a Lagrangian tracer study performed on the west Florida shelf by Wanninkhof et al. (1997) suggest that about 80% of the increase in DIC was due to plankton respiration and the remaining 20% of the increase in DIC was caused by air-sea CO_2 exchange. However, the drivers of long-term deoxygenation in the Florida Straits haven't been studied yet. We presume that the increase in aerobic respiration accounts for the long-term DO decline, considering the concurrence of DO decrease and DIC increase as well as the linear coefficient (−0.625) between DO and DIC. Based on the aerobic respiration equation, 1 mol O_2 consumption leads to 0.768 mol DIC increase (=106/138; Cai et al., 2021). Following this hypothesis, approximately 81% (=0.625/0.768) of the DIC increase is caused by DO decrease.

For the entire Florida Straits at 27°N from 2002 to 2018, the long-term trend of increase in DIC is larger than the trend in ΔDIC_{ant}. The anthropogenic carbon accounted for 85% (=ΔDIC_{ant} trend/DIC trend × 100% = 1.04/

1.23 × 100%) of the long-term increase in DIC while the long-term decrease in DO accounted for 26% (=DO trend × correlation coefficient/DIC trend × 100% = (−0.52) × (−0.625)/1.23 × 100%) of the long-term increase in DIC. In addition, the long-term increasing rate in DIC is highest in NACW as a result of the highest decreasing rate in DO in this water mass. Though the trend in temperature is not statistically significant, the slight increase in temperature leads to a slight decrease (9% = temperature trend × correlation coefficient/DIC trend × 100% = 0.0103 × (−10.4788)/1.23 × 100%) in the long-term change of DIC. The non-significant negative trend in salinity has a minor influence and accounts for 2% (=salinity trend × correlation coefficient/DIC trend × 100% = −0.0007 × 35.4297/1.23 × 100%) of the long-term decrease in DIC during 2002–2018.

In the surface mixed layer, the uptake of atmospheric CO_2 and the resulted increase in ΔDIC_{ant} are major contributors to the long-term DIC increase in the Florida Straits at 27°N. In subsurface waters, microbial respiration, which consumes oxygen and produces CO_2, is an important internal source of DIC in subsurface water. Therefore, the observed long-term DO decrease in the Florida Straits at 27°N plays an important role in the long-term DIC increase in the study region. In NACW where the long-term decreasing rate in DO is highest, the corresponding increasing rate in DIC is also highest due to a higher respiration rate compare to those in SW and AAIW.

Though the long-term trend in DIC is larger than the trend in ΔDIC_{ant}, the long-term trend of DIC transport is not statistically significant while the trend in ΔDIC_{ant} transport is significant. This insignificant trend in DIC transport is primarily a result of the larger short-term variability compared to that in ΔDIC_{ant} transport. That is to say, the signal-to-noise ratio of DIC transport is higher so that it takes a longer time for the long-term trend to be statistically significant.

Similar to the long-term DIC changes, the negative Ω_{arag} trend is highest in NACW and lowest in SW. Interestingly, the highest pH rate of decline is found in AAIW rather than NACW. The reasons are twofold. First, the temperature decline in NACW (-0.03°C yr^{-1}, $p = 0.06$, Figure 4a), which leads to a pH increase when other DIC and TA are constant, compensates for part of the pH decline caused by DIC increase. By removing the temperature trend, the decreasing rate in pH comes to -0.0035 ± 0.0002 yr^{-1} (identical to that of AAIW), which is 17% higher than the determined rate. Second, the buffer capacity of NACW is larger than that of AAIW. $\beta_{DIC}{}^{-1}$, which represents the fractional change in pH over the fractional change in DIC (Egleston et al., 2010), of NACW (4.5 mM^{-1}) is smaller than that of AAIW (6.1 mM^{-1}). Therefore, the rate of decline for NACW pH is lower than that of AAIW, despite its increasing rate in DIC being the highest.

Finally, we compare the long-term pH change in SW of the Florida Straits with those in the greater northern Caribbean Sea SW from 2002 to 2018 using the time series data product contributed by Wanninkhof et al. (2020). Note that the upper 50 m of SW carbonate chemistry data are calculated using MLRs provided by Wanninkhof et al. (2020). The overall decline in SW pH of the northern Caribbean Sea (-0.0030 ± 0.0003 yr^{-1}) is higher than that of SW in the Florida Straits (-0.0026 ± 0.0002 yr^{-1}). Our analysis indicates that the lower net decline in pH within the Florida Straits relative to the northern Caribbean Sea is mainly caused by higher TA from late 2012 to 2018 due to salinity increase during this period (Figure S9 in Supporting Information S1).

4.3. Short-Term Variability

The short-term correlations between volume transport and carbonate chemistry properties can be explained by how much the carbonate chemistry properties of local SW water are being affected by the feed waters of the Loop Current, which is characterized by a relatively low DIC compared to that in surrounding waters (Gomez et al., 2020; Wanninkhof et al., 2015). In SW, when the alongshore velocity is high, more relatively low DIC waters are being transported northward from the Caribbean Sea by the Loop Current. Therefore, the carbonate chemistry of SW water in Florida Straits at 27°N is strongly affected by and thus negatively correlated with volume transport.

5. Conclusion

To study the influence of water transport on carbon parameters in the Florida Strait, we reconstruct seasonal time series data using seasonal hydrographic parameters for DIC, pH, and Ω_{arag} from 2002 to 2018 via a MLR approach developed based on data collected from limited carbonate chemistry focused research cruises. Data for the entire water column suggest that DO, pH, and Ω_{arag} generally decrease with depth across the Florida Strait while DIC increases with depth. Since 2002, the overall DO, pH, and Ω_{arag} are decreasing while DIC is increasing

in the Florida Strait. In terms of temporal changes, short-term variations in DO and DIC are strongly correlated with northward volume transport across the Florida Straits. The largest long-term trends are usually found in NACW where aerobic respiration, an important internal source of DIC, is highest. The long-term pH and Ω_{arag} decreases in AAIW have the potential to threaten the health of living corals, particularly those growing in the bottom waters on the eastern side of the Florida Strait.

Data Availability Statement

The hydrographic, DO, and Florida Current transport data are available at http://www.aoml.noaa.gov/phod/floridacurrent/. Bottle data from GOMECC and ECOA cruises are available at https://www.ncei.noaa.gov/access/ocean-acidification-data-stewardship-oads/synthesis/NAcruises.html. Data from RB-03 and RB-06 cruises are available at https://www.aoml.noaa.gov/ocd/ocdweb/shortcruises/shortcruises_gomcaribbean.html. Data from the A05 cruise are available at https://www.ncei.noaa.gov/access/ocean-carbon-data-system/oceans/woce_a05.html. DIC, pH, and Ω_{arag} time series data generated for this work are available at National Centers for Environmental Information (NCEI) at https://www.ncei.noaa.gov/data/oceans/ncei/ocads/metadata/0244859.html.

Acknowledgments
We thank Dr. Fabian A. Gomez and Dr. Sang-Ki Lee for their helpful comments and suggestions on this manuscript. The authors gratefully acknowledge the NOAA Global Ocean Monitoring and Observing (GOMO) program and the NOAA Ocean Acidification Program (OAP) for support of the carbonate chemistry focused research cruises. This research was carried out in part under the auspices of the Cooperative Institute for Marine and Atmospheric Studies (CIMAS), a Cooperative Institute of the University of Miami and the National Oceanic and Atmospheric Administration, cooperative agreement #NA20OAR4320472.

References

Alin, S. R., Feely, R. A., Dickson, A. G., Hernández Ayón, J. M., Juranek, L. W., Ohman, M. D., & Goericke, R. (2012). Robust empirical relationships for estimating the carbonate system in the southern California Current System and application to CalCOFI hydrographic cruise data (2005-2011). *Journal of Geophysical Research*, *117*(C5), C05033. https://doi.org/10.1029/2011JC007511

Álvarez, M., Sanleón-Bartolomé, H., Tanhua, T., Mintrop, L., Luchetta, A., Cantoni, C., et al. (2014). The CO_2 system in the Mediterranean Sea: A basin wide perspective. *Ocean Science*, *10*(1), 69–92. https://doi.org/10.5194/os-10-69-2014

Baringer, M. O. N., & Larsen, J. C. (2001). Sixteen years of Florida current transport at 27°N. *Geophysical Research Letters*, *28*(16), 3179–3182. https://doi.org/10.1029/2001GL013246

Beal, L. M., Hummon, J. M., Williams, E., Brown, O. B., Baringer, W., & Kearns, E. J. (2008). Five years of Florida Current structure and transport from the Royal Caribbean cruise ship *Explorer of the Seas*. *Journal of Geophysical Research*, *113*(C6), C06001. https://doi.org/10.1029/2007JC004154

Boulais, M., Chenevert, K. J., Demey, A. T., Darrow, E. S., Robison, M. R., Roberts, J. P., & Volety, A. (2017). Oyster reproduction is compromised by acidification experienced seasonally in coastal regions. *Scientific Reports*, *7*(1), 13276. https://doi.org/10.1038/s41598-017-13480-3

Breitburg, D., Levin, L. A., Oschlies, A., Gregoire, M., Chavez, F. P., Conley, D. J., et al. (2018). Declining oxygen in the global ocean and coastal waters. *Science*, *359*(6371), eaam7240. https://doi.org/10.1126/science.aam7240

Brown, P. J., McDonagh, E. L., Sanders, R., Watson, A. J., Wanninkhof, R., King, B. A., et al. (2021). Circulation-driven variability of Atlantic anthropogenic carbon transports and uptake. *Nature Geoscience*, *14*(8), 571–557. https://doi.org/10.1038/s41561-021-00774-5

Cai, W.-J., Feely, R. A., Testa, J. M., Li, M., Evans, W., Alin, S. R., et al. (2021). Natural and anthropogenic drivers of acidification in large Estuaries. *Annual Review of Marine Science*, *13*(1), 23–55. https://doi.org/10.1146/annurev-marine-010419-011004

Carpenter, J. H. (1965). The Chesapeake Bay Institute technique for the Winkler dissolved oxygen method. *Limnology & Oceanography*, *10*(1), 141–143. https://doi.org/10.4319/lo.1965.10.1.0141

Carter, B. R., Bittig, H. C., Fassbender, A. J., Sharp, J. D., Takeshita, Y., Xu, Y.-Y., et al. (2021). New and updated global empirical seawater property estimation routines. *Limnology and Oceanography: Methods*, *19*(12), 785–809. https://doi.org/10.1002/lom3.10461

Carter, B. R., Williams, N. L., Gray, A. R., & Feely, R. A. (2016). Locally interpolated alkalinity regression for global alkalinity estimation. *Limnology and Oceanography: Methods*, *14*(4), 268–277. https://doi.org/10.1002/lom3.10087

Cohen, A. L., & Holcomb, M. (2009). Why corals care about ocean acidification: Uncovering the mechanism. *Oceanography*, *22*(4), 118–127. https://doi.org/10.5670/oceanog.2009.102

Dickson, A. G. (1990). Standard potential of the reaction: AgCl(s) + $1/2H_2$(g) = Ag(s) + HCl(aq), and the standard acidity constant of the ion HSO_4^- in synthetic sea water from 273.15 to 318.15 K. *The Journal of Chemical Thermodynamics*, *22*(2), 113–127. https://doi.org/10.1016/0021-9614(90)90074-Z

Dickson, A. G. (2001). Reference materials for oceanic CO_2 measurements. *Oceanography*, *14*, 21–22.

Dickson, A. G., Sabine, C. L., & Christian, J. R. (2007). Guide to best practices for ocean CO_2 measurements. *PICES Special Publication*, *3*. https://doi.org/10.25607/OBP-1342

Egleston, E. S., Sabine, C. L., & Morel, F. M. M. (2010). Revelle revisited: Buffer factors that quantify the response of ocean chemistry to changes in DIC and alkalinity. *Global Biogeochemical Cycles*, *24*(1). https://doi.org/10.1029/2008GB003407

Franke, G. R. (2010). *Multicollinearity*. Wiley International Encyclopedia of Marketing. edited. https://doi.org/10.1002/9781444316568.wiem02066

Friedlingstein, P., Jones, M. W., O'Sullivan, M., Andrew, R. M., Bakker, D. C. E., Hauck, J., et al. (2022). Global carbon budget 2021. *Earth System Science Data*, *14*(4), 1917–2005. https://doi.org/10.5194/essd-14-1917-2022

Friis, K., Körtzinger, A., Pätsch, J., & Wallace, D. W. R. (2005). On the temporal increase of anthropogenic CO_2 in the subpolar North Atlantic. *Deep-Sea Research I*, *52*(5), 681–698. https://doi.org/10.1016/j.dsr.2004.11.017

Garcia, R. F., & Meinen, C. S. (2014). Accuracy of Florida Current volume transport measurements at 27°N using multiple observational techniques. *Journal of Atmospheric and Oceanic Technology*, *31*(5), 1169–1180. https://doi.org/10.1175/jtech-d-13-00148.1

Gomez, F. A., Wanninkhof, R., Barbero, L., Lee, S.-K., & Hernandez, F. J., Jr. (2020). Seasonal patterns of surface inorganic carbon system variables in the Gulf of Mexico inferred from a regional high-resolution ocean biogeochemical model. *Biogeosciences*, *17*(6), 1685–1700. https://doi.org/10.5194/bg-17-1685-2020

Hoegh-Guldberg, O., Mumby, P. J., Hooten, A. J., Steneck, R. S., Greenfield, P., Gomez, E., et al. (2007). Coral reefs under rapid climate change and ocean acidification. *Science*, *318*(5857), 1737–1742. https://doi.org/10.1126/science.1152509

Iudicone, D., Rodgers, K. B., Plancherel, Y., Aumont, O., Ito, T., Key, R. M., et al. (2016). The formation of the ocean's anthropogenic carbon reservoir. *Scientific Reports*, *6*(1), 35473. https://doi.org/10.1038/srep35473

Jiang, M., Pan, C., Barbero, L., Reed, J., Salisbury, J. E., Vanzwieten, J. H., & Wanninkhof, R. (2020). Variability of bottom carbonate chemistry over the deep coral reefs in the Florida Straits and the impacts of mesoscale processes. *Ocean Modelling*, *147*, 101555. https://doi.org/10.1016/j.ocemod.2019.101555

Jin, P., Hutchins, D. A., & Gao, K. (2020). The impacts of ocean acidification on marine food quality and its potential food chain consequences. *Frontiers in Marine Science*, *7*, 780. https://doi.org/10.3389/fmars.2020.543979

Johnson, K. M., Wills, K. D., Butler, D. B., Johnson, W. K., & Wong, C. S. (1993). Coulometric total carbon dioxide analysis for marine studies: Maximizing the performance of an automated gas extraction system and coulometric detector. *Marine Chemistry*, *44*(2), 167–187. https://doi.org/10.1016/0304-4203(93)90201-X

Kaniewska, P., Campbell, P. R., Kline, D. I., Rodriguez-Lanetty, M., Miller, D. J., Dove, S., & Hoegh-Guldberg, O. (2012). Major cellular and physiological impacts of ocean acidification on a reef building coral. *PLoS One*, *7*(4), e34659. https://doi.org/10.1371/journal.pone.0034659

Langdon, C. (2010). *Determination of dissolved oxygen in seawater by Winkler titration using the amperometric technique*. IOCCP Report No. 14, ICPO Publication Series No. 134.

Larsen, J., & Smith, F. T. (1992). Transport and heat flux of the Florida Current at 27°N derived from cross-stream voltages and profiling data: Theory and observations. *Deep Sea Research Part I: Oceanographic Research Papers*, *338*(1650), 169–236. https://doi.org/10.1098/rsta.1992.0007

Larsen, J. C., & Sanford, T. B. (1985). Florida Current volume transport from voltage measurements. *Science*, *227*(4684), 302–304. https://doi.org/10.1126/science.227.4684.302

Leaman, K. D., Molinari, R. L., & Vertes, P. S. (1987). Structure and variability of the Florida Current at 27°N: April 1982–July 1984. *Journal of Physical Oceanography*, *17*(5), 565–583. https://doi.org/10.1175/1520-0485(1987)017<0565:savotf>2.0.co;2

Lee, K., Kim, T.-W., Byrne, R. H., Millero, F. J., Feely, R. A., & Liu, Y.-M. (2010). The universal ratio of boron to chlorinity for the North Pacific and North Atlantic oceans. *Geochimica et Cosmochimica Acta*, *74*(6), 1801–1811. https://doi.org/10.1016/j.gca.2009.12.027

Lee, T. N., Rooth, C., Williams, E., McGowan, M., Szmant, A. F., & Clarke, M. E. (1992). Influence of Florida Current, gyres and wind-driven circulation on transport of larvae and recruitment in the Florida Keys coral reefs. *Continental Shelf Research*, *12*(7), 971–1002. https://doi.org/10.1016/0278-4343(92)90055-O

Lueker, T. J., Dickson, A. G., & Keeling, C. D. (2000). Ocean pCO_2 calculated from dissolved inorganic carbon, alkalinity, and equations for K_1 and K_2: Validation based on laboratory measurements of CO_2 in gas and seawater at equilibrium. *Marine Chemistry*, *70*(1–3), 105–119. https://doi.org/10.1016/S0304-4203(00)00022-0

Lynch-Stieglitz, J. (2017). The Atlantic meridional overturning circulation and abrupt climate change. *Annual Review of Marine Science*, *9*(1), 83–104. https://doi.org/10.1146/annurev-marine-010816-060415

Macdonald, A. M., Baringer, M. O., Wanninkhof, R., Lee, K., & Wallace, D. W. R. (2003). A 1998–1992 comparison of inorganic carbon and its transport across 24.5°N in the Atlantic. *Deep Sea Research Part II: Topical Studies in Oceanography*, *50*(22), 3041–3064. https://doi.org/10.1016/j.dsr2.2003.07.009

McCarthy, G. D., Smeed, D. A., Johns, W. E., Frajka-Williams, E., Moat, B. I., Rayner, D., et al. (2015). Measuring the Atlantic meridional overturning circulation at 26°N. *Progress in Oceanography*, *130*, 91–111. https://doi.org/10.1016/j.pocean.2014.10.006

McGarry, K. S. A., Salisbury, J., Salisbury, J., & Alin, S. R. (2021). Multiple linear regression models for reconstructing and exploring processes controlling the carbonate system of the Northeast US from basic hydrographic data. *Journal of Geophysical Research: Oceans*, *126*(2), e2020JC016480. https://doi.org/10.1029/2020JC016480

Meinen, C. S., Baringer, M. O., & Garcia, R. F. (2010). Florida Current transport variability: An analysis of annual and longer-period signals. *Deep Sea Research Part I: Oceanographic Research Papers*, *57*(7), 835–846. https://doi.org/10.1016/j.dsr.2010.04.001

Mollica, N. R., Guo, W., Cohen, A. L., Huang, K.-F., Foster, G. L., Donald, H. K., & Solow, A. R. (2018). Ocean acidification affects coral growth by reducing skeletal density. *Proceedings of the National Academy of Sciences*, *115*(8), 1754–1759. https://doi.org/10.1073/pnas.1712806115

Morey, S., Koch, M., Liu, Y., & Lee, S.-K. (2017). Florida's oceans and marine habitats in a changing climate. *Florida's Climate: Changes, Variations, & Impacts*, 391–425. Chapter 13. https://doi.org/10.1725/fci2018.ch13

Rosón, G., Ríos, A. F., Pérez, F. F., Lavín, A., & Bryden, H. L. (2003). Carbon distribution, fluxes, and budgets in the subtropical North Atlantic Ocean (24.5°N). *Journal of Geophysical Research*, *108*(C5), 3144. https://doi.org/10.1029/1999JC000047

Sarmiento, J. L., Murnane, R. J., & Quéré, C. L. (1995). Air-sea CO_2 transfer and the carbon budget of the North Atlantic. *Philosophical Transactions of the Royal Society B*, *348*, 211–219. https://doi.org/10.1098/RSTB.1995.0063

Schmitz, W. J., & Richardson, P. L. (1991). On the sources of the Florida Current. *Deep-Sea Research, Part A: Oceanographic Research Papers*, *38*, S379–S409. https://doi.org/10.1016/S0198-0149(12)80018-5

Smeed, D. A., Josey, S. A., Beaulieu, C., Johns, W. E., Moat, B. I., Frajka-Williams, E., et al. (2018). The North Atlantic Ocean is in a state of reduced overturning. *Geophysical Research Letters*, *45*(3), 1527–1533. https://doi.org/10.1002/2017GL076350

Smeed, D. A., McCarthy, G. D., Cunningham, S. A., Frajka-Williams, E., Rayner, D., Johns, W. E., et al. (2014). Observed decline of the Atlantic meridional overturning circulation 2004-2012. *Ocean Science*, *10*(1), 29–38. https://doi.org/10.5194/os-10-29-2014

Sponaugle, S., Lee, T., Kourafalou, V., & Pinkard, D. (2005). Florida Current frontal eddies and the settlement of coral reef fishes. *Limnology & Oceanography*, *50*(4), 1033–1048. https://doi.org/10.4319/lo.2005.50.4.1033

Szuts, Z. B., & Meinen, C. S. (2017). Florida Current salinity and salinity transport: Mean and decadal changes. *Geophysical Research Letters*, *44*(20), 10495–10503. https://doi.org/10.1002/2017GL074538

Takahashi, T., Sutherland, S. C., Wanninkhof, R., Sweeney, C., Feely, R. A., Chipman, D. W., et al. (2009). Climatological mean and decadal change in surface ocean pCO_2, and net sea–air CO_2 flux over the global oceans. *Deep Sea Research Part II: Topical Studies in Oceanography*, *56*(8), 554–577. https://doi.org/10.1016/j.dsr2.2008.12.009

Talley, L. D., Pickard, G. L., Emery, W. J., & Swift, J. H. (2011). *Descriptive physical oceanography: An introduction* (6th ed.). Elsevier.

Van Heuven, S., Pierrot, D., Rae, J. W. B., & Wallace, D. W. R. (2009). *MATLAB program developed for CO_2 system calculations*. Carbon Dioxide Information Analysis Center, Oak Ridge National Laboratory, U.S. Department of Energy. https://doi.org/10.3334/CDIAC/otg.CO2SYS_MATLAB_v1.1

Wanninkhof, R., Barbero, L., Byrne, R., Cai, W.-J., Huang, W.-J., Zhang, J.-Z., et al. (2015). Ocean acidification along the Gulf Coast and East Coast of the USA. *Continental Shelf Research*, *98*, 54–71. https://doi.org/10.1016/j.csr.2015.02.008

Wanninkhof, R., Hitchcock, G., Wiseman, W. J., Vargo, G., Ortner, P. B., Asher, W., et al. (1997). Gas exchange, dispersion, and biological productivity on the West Florida Shelf: Results from a Lagrangian tracer study. *Geophysical Research Letters*, *24*(14), 1767–1770. https://doi.org/10.1029/97GL01757

Wanninkhof, R., Pierrot, D., Sullivan, L., Barbero, L., & Triñanes, J. (2020). A 17-year dataset of surface water fugacity of CO_2 along with calculated pH, aragonite saturation state and air-sea CO_2 fluxes in the northern Caribbean Sea. *Earth System Science Data*, *12*(3), 1489–1509. https://doi.org/10.5194/essd-12-1489-2020

Wanninkhof, R., Triñanes, J., Park, G.-H., Gledhill, D., & Olsen, A. (2019). Large decadal changes in air-sea CO_2 fluxes in the Caribbean Sea. *Journal of Geophysical Research: Oceans*, *124*(10), 6960–6982. https://doi.org/10.1029/2019JC015366

Wennekens, M. P. (1959). Water mass properties of the Straits of Florida and related waters. *Bulletin of Marine Science of the Gulf and Caribbean*, *9*(1), 1–52.

Whiteley, N. M. (2011). Physiological and ecological responses of crustaceans to ocean acidification. *Marine Ecology Progress Series*, *430*, 257–272. https://doi.org/10.3354/meps09185

Zhang, L. N., & Woosley, R. J. (2021). Seasonal trends in the Southeast Florida current and shelf CO_2 fluxes. *Continental Shelf Research*, *229*, 104566. https://doi.org/10.1016/j.csr.2021.104566